

AD_____

Award Number: W81XWH-11-1-0167

TITLE: Mechanism-Based Enhanced Delivery of Drug-Loaded Targeted Nanoparticles
for Breast Cancer Therapy

PRINCIPAL INVESTIGATOR: Tatiana Bronich, Ph.D.

CONTRACTING ORGANIZATION: University of Nebraska
Omaha, NE 68198-7835

REPORT DATE: February 2012

TYPE OF REPORT: Annual

PREPARED FOR: U.S. Army Medical Research and Materiel Command
Fort Detrick, Maryland 21702-5012

DISTRIBUTION STATEMENT: Approved for Public Release;
Distribution Unlimited

The views, opinions and/or findings contained in this report are those of the author(s) and should not be construed as an official Department of the Army position, policy or decision unless so designated by other documentation.

REPORT DOCUMENTATION PAGE				Form Approved OMB No. 0704-0188	
Public reporting burden for this collection of information is estimated to average 1 hour per response, including the time for reviewing instructions, searching existing data sources, gathering and maintaining the data needed, and completing and reviewing this collection of information. Send comments regarding this burden estimate or any other aspect of this collection of information, including suggestions for reducing this burden to Department of Defense, Washington Headquarters Services, Directorate for Information Operations and Reports (0704-0188), 1215 Jefferson Davis Highway, Suite 1204, Arlington, VA 22202-4302. Respondents should be aware that notwithstanding any other provision of law, no person shall be subject to any penalty for failing to comply with a collection of information if it does not display a currently valid OMB control number. PLEASE DO NOT RETURN YOUR FORM TO THE ABOVE ADDRESS.					
1. REPORT DATE February 2012		2. REPORT TYPE Annual		3. DATES COVERED 18 January 2011 – 17 January 2012	
4. TITLE AND SUBTITLE Mechanism-Based Enhanced Delivery of Drug-Loaded Targeted Nanoparticles for Breast Cancer Therapy				5a. CONTRACT NUMBER	
				5b. GRANT NUMBER W81XWH-11-1-0167	
				5c. PROGRAM ELEMENT NUMBER	
6. AUTHOR(S) Tatiana Bronich E-Mail: tbronich@unmc.edu				5d. PROJECT NUMBER	
				5e. TASK NUMBER	
				5f. WORK UNIT NUMBER	
7. PERFORMING ORGANIZATION NAME(S) AND ADDRESS(ES) University of Nebraska Omaha, NE 68198-7835				8. PERFORMING ORGANIZATION REPORT NUMBER	
9. SPONSORING / MONITORING AGENCY NAME(S) AND ADDRESS(ES) U.S. Army Medical Research and Materiel Command Fort Detrick, Maryland 21702-5012				10. SPONSOR/MONITOR'S ACRONYM(S)	
				11. SPONSOR/MONITOR'S REPORT NUMBER(S)	
12. DISTRIBUTION / AVAILABILITY STATEMENT Approved for Public Release; Distribution Unlimited					
13. SUPPLEMENTARY NOTES					
14. ABSTRACT This Synergistic IDEA project seeks to develop a novel strategy to effectively target ErbB2-overexpressing breast cancer with anti-ErbB2 antibody coated nanogels carrying potent chemotherapeutics in combination with HSP90 inhibitors to enhance the endocytosis of ErbB2-receptor bound nanogel cargo. A successful outcome of our studies will provide a new therapeutic approach against a particularly difficult form of breast cancer and may provide a template for therapeutic targeting of other forms of breast cancer and other cancers. Success in preclinical models would also provide strong rationale for clinical translation of this technology with the ultimate goals of selective delivery of imaging and therapeutic modalities to tumors. Robust procedures for the synthesis of nanogels were developed, key structural parameters of block copolymers governing the physicochemical properties of the nanogels were identified, nanogels loaded with combination of anticancer therapeutics and methods for the preparation of ErbB2-targeted nanogels were developed, Mannose functionalized BICs provided a safe and stable platform for gene delivery to macrophages, doxorubicin-nanogels showed an efficient systemic drug delivery to human tumor xenografts.					
15. SUBJECT TERMS Nanoparticles breast cancer therapy					
16. SECURITY CLASSIFICATION OF:			17. LIMITATION OF ABSTRACT UU	18. NUMBER OF PAGES 13	19a. NAME OF RESPONSIBLE PERSON USAMRMC
a. REPORT U	b. ABSTRACT U	c. THIS PAGE U			19b. TELEPHONE NUMBER (include area code)

Table of Contents

	<u>Page</u>
Introduction.....	4
Body.....	4
Key Research Accomplishments.....	11
Reportable Outcomes.....	12
Conclusion.....	12
References.....	12
Appendices.....	N/A

2011-2012 Annual Report

Project BC102673: Mechanism-based enhanced delivery of drug-loaded targeted nanoparticles for breast cancer therapy

(Contract Number W81WH-11-1-0167)

PI: Dr. Tatiana Bronich

INTRODUCTION

Breast cancer is the second leading type of cancer among women in the U.S. In 2011, there were more than 2.6 million breast cancer survivors and over 230,480 new cases of invasive breast cancer were expected to be diagnosed (<http://www.breastcancer.org>). Nearly a third of breast cancer patients are diagnosed to be positive for the Human Epidermal Growth Factor Receptor 2 (Her2; also known as ErbB2 or Neu) and therefore represent a major therapeutic target. The humanized anti-ErbB2 monoclonal antibody, Trastuzumab (Herceptin™, Genentech, San Francisco, CA), is now an essential part of treatment of ErbB2-overexpressing breast cancers. Trastuzumab is currently administered with other chemotherapeutics, like microtubule stabilizing agents (Docetaxel, Paclitaxel), DNA binding drugs (Doxorubicin, Epirubicin, Cisplatin) or alkylating agents (Cyclophosphamide). However, clinical data indicate a less than satisfactory response rate in patients and importantly, most patients that do respond initially eventually develop resistance. In addition to the tumor cells acquiring resistance, the patients also have to endure the effects of the chemotherapeutics on the normal tissue. Anti-ErbB2 antibody-conjugated polymeric nanoparticles with a capacity to load multiple drugs at high concentrations represent a promising alternative to circumvent these problems. However, success of ErbB2-targeted drug-delivery into the cytosol using nanotechnology platforms, similar to nanoparticles in general, critically depends on the efficiency of internalization. Optimal targeting must therefore take into account the biology of endocytic trafficking of ErbB2 receptor. Specifically, the low rate of endocytosis is attributed to constitutive association of ErbB2 with Heat Shock Protein 90 (HSP90). This Synergistic IDEA project seeks to develop a novel strategy to effectively target ErbB2-overexpressing breast cancer with anti-ErbB2 antibody coated nanogels carrying potent chemotherapeutics in combination with HSP90 inhibitors to enhance the endocytosis of ErbB2-receptor bound nanogel cargo. A successful outcome of our studies will provide a new therapeutic approach against a particularly difficult form of breast cancer and may provide a template for therapeutic targeting of other forms of breast cancer and other cancers. Success in preclinical models would also provide strong rationale for clinical translation of this technology with the ultimate goals of selective delivery of imaging and therapeutic modalities to tumors.

BODY OF REPORT

This section describes the efforts devoted by the Dr. Bronich research team to meet the major technical objectives that were: (i) synthesis and characterization of nanogels with cross-linked ionic cores from poly(carboxylic acid) chains and a hydrophilic shell from poly(ethylene oxide) (PEO) chains, (ii) optimization of the structure and composition of drug-loaded nanogels; (iii) develop the procedures for conjugation of anti-ErbB2 antibody (Trastuzumab) to nanogels; (iv) *in vivo* "proof of concept" drug release studies using an animal tumor model.

Synthesis of nanogels. Cross-linked nanogels were prepared by template-assisted method using a two-step process, which includes 1) condensation of block ionomers with Ca^{2+} ions into spherical self-assembled block ionomer complexes (BIC) and 2) cross-linking reaction of BIC templates by bifunctional agents using the procedure described in our previous reports and publications [1-3]. Doubly hydrophilic copolymers containing anionic and nonionic hydrophilic polymeric segments (block ionomers) were used for the synthesis of nanogels. Polymethacrylic acid (PMA) and polyglutamic acid (PGA) were used as anionic blocks. Poly(ethylene oxide), PEO, was used as a hydrophilic block. The characteristics of block copolymers used in these studies are summarized in Table 1. Diblock copolymer samples are denoted as PEO(x)-b-PMA(y) or PEO(x)-b-PGA(y), where x and y

represent the degree of polymerization of the PEO segment and PMA or PGA segment, respectively.

Nanogels were synthesized using the general procedure as was described earlier [3]. Briefly, PEO-*b*-PMA/ Ca^{2+}

Table 1. Characteristics of block copolymers

Block copolymer ^a	Molecular weight	Polydispersity index
PEO(170)- <i>b</i> -PMA(180)	23,000	1.45
PEO(125)- <i>b</i> -PMA(180)	21,000	1.16
PEO(114)- <i>b</i> -PGA(100)	20,600	1.22
PEO(114)- <i>b</i> -PGA(150)	27,500	1.38

^aThe average number of ethylene oxide and carboxylic acid units (in parentheses) in block copolymers were calculated using the average molecular weights provided by manufacturer

complexes were prepared by mixing an aqueous solution of PEO(170)-*b*-PMA(180) with a solution of CaCl_2 at a molar ratio of $[\text{Ca}^{2+}]/[\text{COO}^-]=1.1$. The inner core of the micelles formed was cross-linked through the carboxylic groups using bifunctional agent, 1,2-ethylenediamine, in the presence of 1-(3-dimethylaminopropyl)-3-ethylcarbodiimide hydrochloride (EDC) at appropriate molar ratios to achieve the desired theoretical extent of cross-linking. The theoretical extent of cross-linking has been controlled by the ratio of amine functional groups to carboxylic acid groups of block-polymer. It should be noted, that actual extent of cross-linking were expected to be significantly less [1], due to side reaction between water and the activated carboxylic groups. Moreover, it is quite likely that some portion of the diamine could form a “loop” being bound to the same PMA chain as well as attach by one amino group giving the free amine. It has been estimated that approximately two cross-links per block copolymer chain were formed in the micelles with targeted 20% degree of cross-linking. The reaction mixture was allowed to stir overnight at room temperature. The byproducts of the cross-linking reaction and metal ions were removed by exhaustive dialysis of the reaction mixtures, against (1) 0.5% aqueous ammonia in the presence of ethylenediaminetetraacetic acid (EDTA), and (2) distilled water. The resulting nanogels were of ca. 130 nm in diameter and had a net negative charge (ζ -potential = -22 mV). The core of such micelles comprised a swollen network of the cross-linked PMA chains and was surrounded by the shell of hydrophilic PEO chains. The hydrogel-like behavior of these micelles was observed upon a change of pH. Their size increased considerably with increasing pH, which was completely reversible. The particles were stable and revealed no size change even upon a 100-fold dilution.

We explored the effects of the hydrophobicity and the length of cross-linker on the structure and swelling properties of the cross-linked micelles using several diamino cross-linkers. 1,2-ethylenediamine, 1,5-diaminopentane, cystamine HCl, and 2,2'-(ethylenedioxy)bis (ethylamine)

were used to cross-link the cores of template PEO(170)-*b*-PMA(180)/Ca²⁺ micelles with targeted degree of cross-linking from 10% to 60%. The incorporation of more hydrophobic cross-linkers into the core of the micelles resulted in the formation of polymer micelles with smaller sizes (Fig. 1). Conventional solution-state ¹H NMR allowed us to estimate the changes in the extent of cross-linking upon the synthesis. As expected, the number of cross-links introduced into the core of the micelles increased with the increase of targeted degree of cross-linking. Furthermore, the number of cross-links in the micelles was elevated when more hydrophobic cross-linker was used (Fig. 2). As a result the swelling of the core of such micelles upon increase of pH was suppressed: only a modest increase in the D_{eff} was observed for the micelles with hydrophobic cross-linkers (e.g. 1,5-diaminopentane) (Fig. 1).

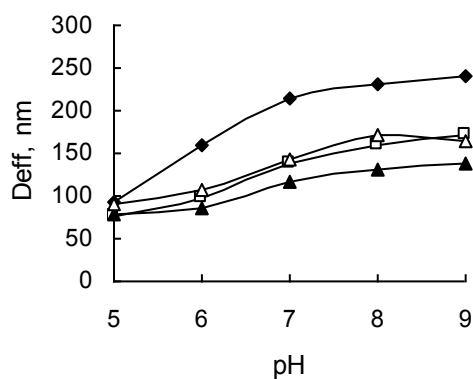


Fig. 1. Effective diameter (D_{eff}) of cross-linked PEO-*b*-PMA micelles at various pH: (◆) ethylenediamine; (□) 1,5-diaminopentane; (▲) cystamine; (△) 2,2'-(ethylenedioxy)-*bis*-(ethylamine).

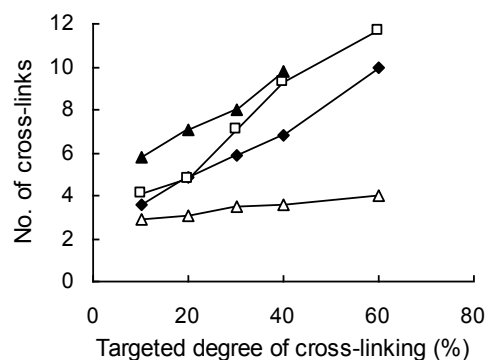


Fig. 2 Relative number of cross-links per chain in PEO-*b*-PMA micelles as a function of targeted degree of cross-linking: (◆) ethylenediamine; (□) 1,5-diaminopentane; (▲) cystamine; (△) 2,2'-(ethylenedioxy)-*bis*-(ethylamine).

Stable biodegradable cross-linked polymer micelles were prepared using PEO-*b*-poly(glutamic acid) block copolymers (PEO(114)-*b*-PGA(100) and PEO(114)-*b*-PGA(150)). In contrast to PEO-*b*-PMA copolymers, PEO-*b*-PGA copolymers were able to form block ionomer complexes only in the presence of metal ions of higher valency such as Al³⁺ or Gd³⁺. The synthesized PEO-*b*-PGA nanogels were of 100-300 nm in diameter and were readily degradable in the presence of proteases. For example, in the presence of ca. 7 units of protease from Bovine pancreas the PEO-*b*-PGA nanogels were degraded within 4 hours at 37°C.

To enable solubilization of the relatively hydrophobic drug 17-AAG into the nanogel core, hydrophobic moieties were introduced into the core-forming segments of PEO(114)-*b*-PGA(150) nanogels. Specifically, PGA block was modified with hydrophobic phenylalanine moieties (Phe) via carbodiimide chemistry using Phe methyl ester (degree of modification was 30% as determined by ¹H NMR). Such amphiphilic copolymer, PEO-*b*-PPGA, readily formed PEG-*b*-PPGA/Ca²⁺ complexes-templates and allowed to prepare polypeptide-based nanogels of small size (ca. 72 nm at pH 7).

Drug-loaded nanogels. A weakly basic drug doxorubicin, DOX, (pK_a = 8.2) was immobilized into the cores of PEO(170)-*b*-PMA(180) nanogels that contain PMA, a weak polyacid (apparent pK_a

is 5.5), by simple mixing of this drug with the aqueous dispersion of the nanogels. Nanogels were prepared using relatively hydrophobic cross-linker, 1,5-diaminopentane (DAP). Briefly, the aqueous solutions of DOX (2 mg/ml) and polymer nanogels were mixed at pH 7 and incubated for 24 h at room temperature. The composition of the mixtures expressed as the feeding molar ratio of DOX to carboxylate groups ($R=[\text{DOX}]/[\text{COO}^-]$) was kept at 0.5. Free unbound DOX was removed thoroughly by repeated filtrations through a 30kDa molecular cutoff membrane pretreated with the drug to retain only the DOX- loaded nanogels. As expected, drug loading was accompanied by a decrease in both the size and net negative charge (ζ -potential) of the nanogels (effective diameter $D_{\text{eff}}=138.9\pm4.3$ nm, ζ -potential = - 34.0 \pm 2.6 mV vs. $D_{\text{eff}}=115.0\pm1.1$ nm, ζ -potential = - 18.1 \pm 3.1 mV for initial and DOX-loaded nanogels). This is consistent with the neutralization of the PMA chains upon DOX binding to carboxylate groups, resulting in reduction of the osmotic swelling pressure inside the cores of nanogels. A substantial drug loading level (up to 50 w/w%) was achieved and it

was strongly dependent on the structure of the nanogels. For example, maximal loading capacity (expressed as mass of incorporated DOX per mass of DOX-loaded nanogels) of nanogels with DAP cross-links and 60% targeted degree of cross-linking was 55.2%, while nanogels with cystamine cross-links and 20% targeted degree of cross-linking exhibited loading capacity of 42.5%. DOX-loaded nanogels maintained their dispersion stability and exhibited no aggregation or precipitation for a prolonged period of time (up to several months). It is of interest to note that binding of DOX to the PEO-b-PGA nanogels, resulted in the formation of large aggregates with low dispersion stability, perhaps, because the resulting DOX/PGA

complex was too hydrophobic and the PEO segments in the corona of the nanogels were unable to stabilize the particles in dispersion. The release profiles were examined for DOX-loaded nanogels with various cross-links in the core to address the effect of the nanogel structure on DOX release. All types of micelles displayed sustained release of DOX under physiological conditions and no burst release was observed. Of particular interest was the finding that the rate at which DOX was released from the nanogels with more hydrophobic cross-links (DAP, cystamine) in the core was substantially slower (Fig. 3).

To solubilize 17-AAG into DOX-loaded nanogels we used the thin-film dissolution method. Appropriate amount of 17-AAG was dissolved in methanol and after complete removal of the solvent, the films dried in vacuo for at least 3 h to remove residual solvent. Subsequently an

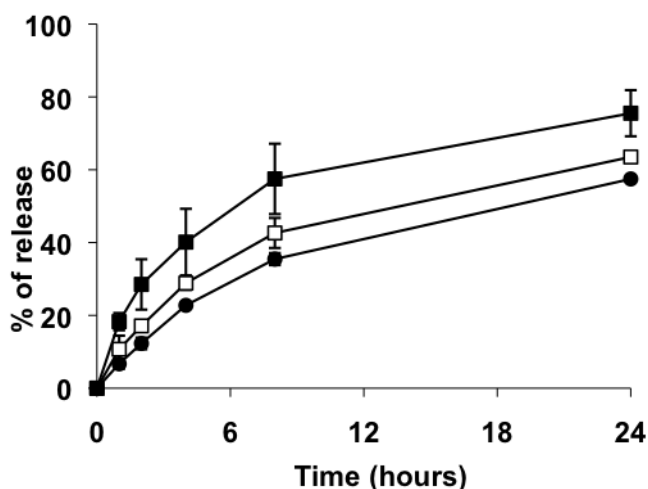


Fig. 3. Release profiles of DOX from PEO-b-PMA nanogels (20% targeted degree of cross-linking) with various cross-links in the cores: ethylenediamine (■); DAP (□); cystamine (●). The loading capacity of DOX for each sample is 200 μ g. The data represent averaged values and standard deviations calculated based on three independent experiments.

aqueous solution of empty or DOX-loaded nanogels were added to the vial and incubated for 24 h. Unbound 17-AAG was removed by filtration through HPLC syringe filters (0.45 mm pore size). The concentration of DOX present in the nanogels was quantified spectrophotometrically using the absorbance at 410 nm. The concentration of 17-AAG was determined by HPLC analysis under isocratic conditions using an Agilent 1200 system. As stationary phase an Agilent Eclipse XDB C18-5 μ m column was used (150 x 4.6 mm), a mobile phase of acetonitrile/10mM ammonium acetate containing 0.1v% acetic acid (pH 4.8) mixture (50/50, v/v) was applied.

Table 2. Physicochemical characteristics of drug-loaded nanogels

Nanogel	Particle size (nm)	PDI	ζ -potential (mV)
PEO-b-PMA	144.5	0.109	-32.8
PEO-b-PMA /DOX	98.6	0.154	-22.1
PEO-b-PMA /DOX+17-AAG	105.9	0.080	-19.7
PPGA	82.5	0.185	-45.5
PPGA /DOX	69.3	0.198	-22.7
PPGA/DOX+17-AAG	57.4	0.161	-21.5

Particle size, polydispersity index (PDI) and ζ -potential were determined by dynamic light scattering at pH 7.0.

whereas it was 1.4:1 w/w for the PPGA nanogels. The physicochemical characteristics of drug-loaded nanogels are presented in Table 1.

The release of drugs from combination formulations in PPGA nanogels was studied in phosphate buffered saline (PBS, pH 7.4, 0.14 M NaCl). We found no notable differences in drug release rate within 24h from combination formulation as compared to single drug formulations. These data suggest that the binary drugs could be delivered and released simultaneously by nanogels.

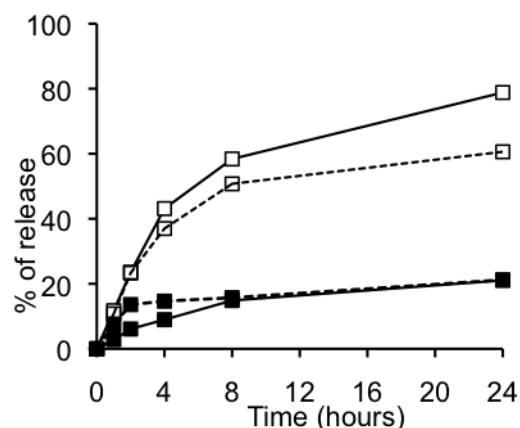


Fig. 4. Drug release profiles for DOX(□) and 17-AAG (■) from combination formulation (solid lines) and single formulation PPGA nanogels (dashed lines) in PBS, pH 7.4.

Synthesis and characterization of anti-ErbB2 antibody (Trastuzumab) modified nanogels. One of the common strategies for immobilization of monoclonal antibodies on the surface of particles is by PEG-linker. In our study mAb (Trast and mouse igG) were attached to the nanogels via a bifunctional NH₂-PEO-MAL cross-linker, which reacts with a carboxylic groups of nanoparticles as well as a thiol group introduced into the antibody. To achieve this, the amino groups from lysine residues of antibody were converted to thiol groups using 2-iminotiolane (Traut's reagent). The thiolated antibodies were conjugated to PEO linker containing 170 repeated units (Mw 7.5 kDa). During pegylation of antibodies all reaction mixture included EDTA to prevent

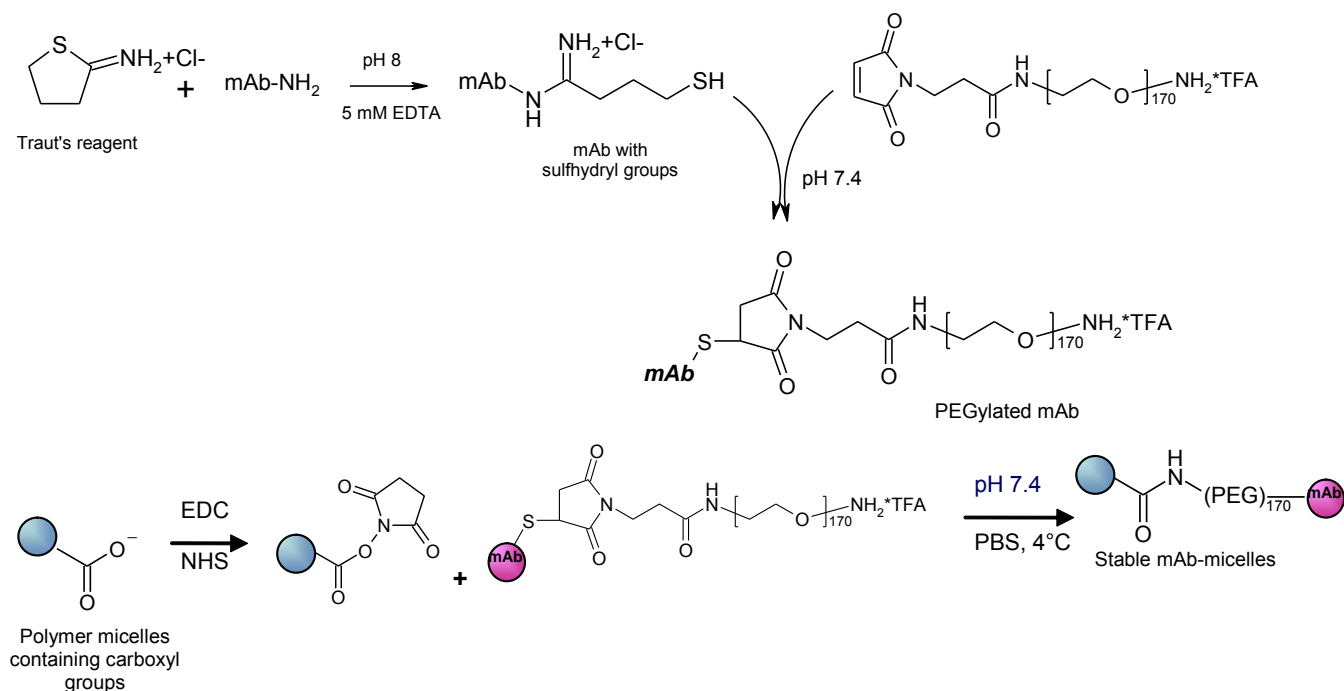


Fig. 5. Scheme of synthesis of mAb conjugated PEG-b-PMA nanogels.

oxidation of sulfhydryls (i.e., formation of disulfide bonds). The pegylated mAbs were conjugated with nanogels via amide linkage between the NHS activated carboxyl groups of micelles and amino groups of mAb-PEG (Fig.5). The Trast-nanogels were purified by SEC on Sepharose CL-6B. This purification procedure allowed removing all unbound mAb, while the unmodified and mAb-conjugated nanogels were not separated. After coupling the size of the particles slightly increased from 160 nm to ca. 180-190 nm. Interestingly, that zeta-potential of Trast-conjugated nanogels increased compare to unmodified particles (e.g. -25 mV vs. -6 mV). Probably, the net negative charge of the modified nanogels was partially shield by additional external PEO chains and mAb. Practically the same results were obtained for nanogels modified with non-specific mouse IgG. The mAb-conjugated nanogels with 60-80 μ g protein per mg of nanogel remained stable in PBS, pH 7.4, exhibiting no aggregation for several weeks. Specific interactions between mAb-modified nanogels and its targeted antigen, ErbB2, on the surface of cancer cells were examined by

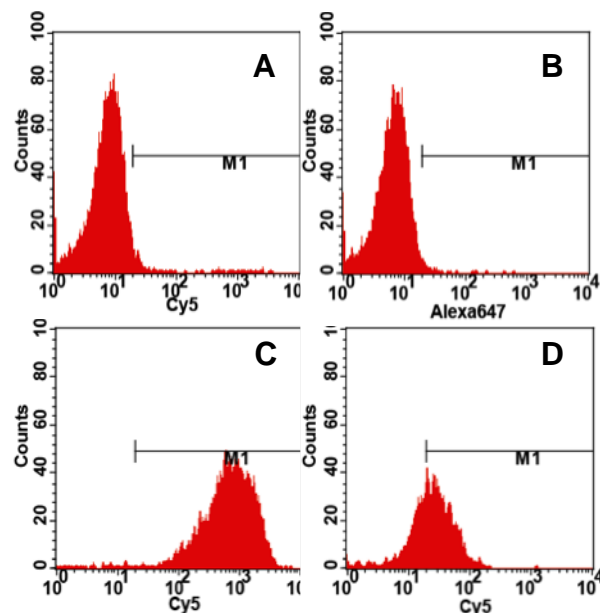


Fig. 6. FACS analysis of binding of Trastuzumab-nanogels to ErbB2-overexpressing breast cancer cells. (A) Cy5-labeled secondary Ab alone; (B) IgG-nanogels (20 μ g/ml) + Alexa 647-antimouse Ab. (C) Trast (10 μ g/ml) + Cy5-Sec; (D) Trast-nanogels (20 μ g/ml) + Cy5-Sec.

flow cytometry and confocal microscopy. We found that the mAb-conjugated nanogels were able to recognize the ErbB2 receptors, however, their binding was significantly less effective compare to free Trastuzumab antibody (Fig.6). Nanogels decorated with unspecific IgG showed no specific binding to the ErbB2 receptor.

Alternatively, mAb were introduced to the surface of nanogels using streptavidin-biotin complex (Fig. 7). Briefly, streptavidin was attached to the nanogels via PEO cross-linker (Mw 10 kDa) followed by conjugation to biotinylated Trast. The final conjugates were purified by SEC (Sephacrose CL-6B). Flow cytometry analysis revealed strong specific binding of these targeted nanogels to ErbB2-

overexpressing breast cancer cells (Fig. 8) comparable to free Trastuzumab antibody. These data suggest that as a result of decoration of the nanogels with the specific antibodies, the Trast-nanogels acquire ability for strong interaction with its targeted antigen.

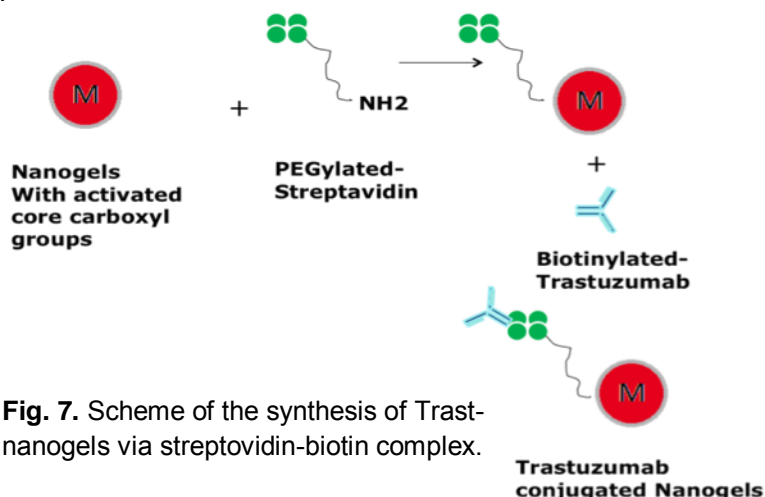


Fig. 7. Scheme of the synthesis of Trast-nanogels via streptavidin-biotin complex.

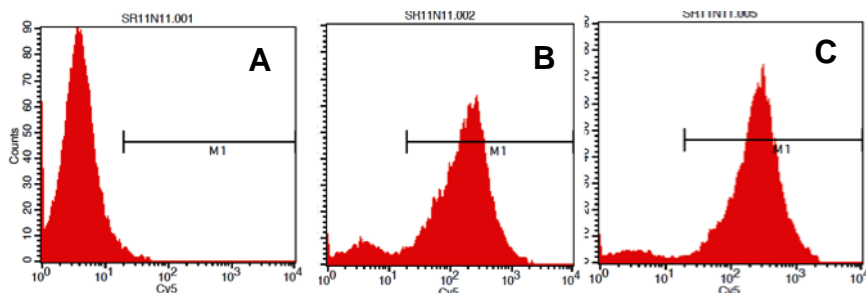


Fig. 7. FACS analysis of binding of Trast-nanogels prepared via streptavidin-biotin complex to ErbB2-overexpressing breast cancer cells. (A) Cy5-labeled secondary Ab alone; (B) biotinylated Trast + Cy5-Sec; (C) Trast- nanogels + Cy5-Sec.

In vivo DOX release from nanogels. Drug release and biodistribution of DOX-loaded nanogels were evaluated in female nude athymic 4 week old mice bearing ectopic A2780 human ovarian cancer xenograft tumor (300-400 mm³) after a single i.v. bolus dose (n=5) of free DOX or DOX-loaded nanogels at 6 mg DOX/kg of animal. The pharmacokinetic profiles of DOX and DOX-loaded nanogels in plasma are presented in Fig.4. Free DOX was rapidly cleared from the blood compartment after i.v. injection. In contrast, the DOX-loaded nanogels showed an initial rapid clearance from the blood, followed by slow clearance after 2h post injection. The plasma concentration of DOX incorporated in nanogels was significantly higher than that of free DOX 2h after injection. The PK parameters were evaluated using noncompartmental analysis with WinNonlin software. An estimated terminal elimination half-life was significantly extended from 5.8h for DOX to 36.9h for DOX-loaded nanogels, while the total clearance of DOX delivered by nanogels was estimated to be 1513.9 ± 335.1 mL/kg/h, four fold less than for free DOX (6039.4 ± 1590.1 mL/kg/h). As a result of reduced plasma clearance, DOX formulated in nanogels

exhibited prolonged blood circulation. Indeed, the area under the plasma concentration - time curve ($AUC_{0 \rightarrow \infty}$) value for DOX-loaded nanogels was four-fold greater than that of free DOX up to 48 h. Nanogels significantly altered tissue distribution of DOX. In particular, tumor accumulation of DOX-loaded nanogels (approximately 1.6 % of injected dose per g tissue) was twice higher than for the free DOX and was maintained at the elevated level for at least 48h. On the other hand, tumor concentrations of DOX were maximal at 5 min post dosing of free DOX and then sharply decreased. $AUC_{0 \rightarrow 48h}$ for DOX-loaded nanogels in the tumor was 2.7-times greater than that of free DOX (Table 2). These data suggest that DOX was effectively delivered to the tumor by means of polymeric nanogels. Furthermore, the DOX concentrations in the heart, kidneys and lungs were significantly reduced by DOX-loaded nanogels, in contrast to the increasing level of DOX in the tumor. It is well known that DOX levels in the heart and kidneys are related to the cardiac toxicity and nephrotoxicity of DOX [4, 5]. The significant reduction in distribution of DOX to heart and kidneys indicates the potential of nanogels in reducing adverse effects associated with DOX therapy. On the other hand, DOX-loaded nanogels were distributed mainly in the organs of the reticuloendothelial system such as the liver and spleen. Such high uptake of nanoparticles in liver and spleen has been reported for other drugs, which are incorporated in polymeric carriers including pegylated liposomes [6,7].

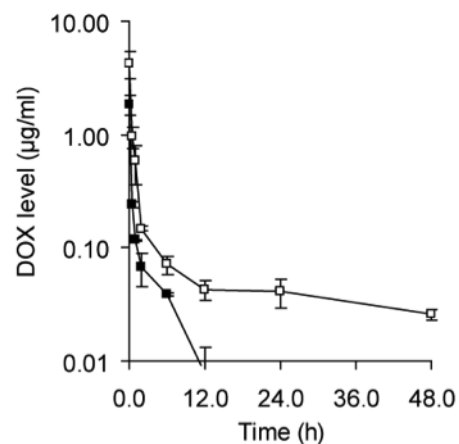


Fig. 4. Pharmacokinetic profiles of free DOX (■) and DOX incorporated into nanogels (○) in the plasma after i.v. injection at a single dose of 6mg/kg. The data represent the mean \pm SD (n=5).

Table 2. Biodistribution of DOX and DOX-loaded cl-micelles after i.v. injection in A2780 tumor-bearing mice at a single dose of 6mg/kg.

Organ	AUC _{0→48h}		AUC ratio ^a
	Free DOX	DOX-loaded nanogels	
Tumor	32	86	2.7
Heart	175	63	0.4
Liver	147	425	2.9
Spleen	218	1601	7.3
Kidney	75	69	0.9
Lung	222	90	0.4

^aAUC ratio = AUC of DOX-loaded nanogels/AUC of free DOX

KEY RESEARCH ACCOMPLISHMENTS

- Representative panel of nanogels was synthesized using diblock copolymers of different structure and compositions.
- The chemical structure of the block copolymer is a key parameter determining the formation of templates for the nanofabrication of nanogels.
- The physicochemical characteristics of the nanogels (dimensions, swelling behavior) can be tuned by changing the cross-linking density of the cores of the nanogels or by using cross-linkers with different chemical structures. The incorporation of more hydrophobic cross-linkers

into the core of the nanogels resulted in the formation of nanogels with smaller sizes and with higher density of cross-links.

- Doxorubicin can be loaded into cross-linked cores of the nanogels with high loading capacity (up to 55 w/w%).
- The nanogels containing drug combinations (doxorubicin and 17-AAG) were prepared and characterized.
- Procedures for conjugation of nanogels with Trastuzumab antibodies in aqueous media were developed.
- “Proof-of-principle” biodistribution studies demonstrated that doxorubicin-nanogels showed an efficient systemic delivery of the drug to human tumor xenografts.

REPORTABLE OUTCOMES

Invited Presentations

1. “Engineering of Soft Nanomaterials for Drug Delivery: Opportunities and Challenges”
University of North Carolina at Chapel Hill, Chapel Hill, NC, July, 2011
2. “Ionic Nanogels as a Versatile Platform for Drug Delivery in Tumor”, 2nd International Summer School “Nanomaterials and Nanotechnologies in Living Systems”, Moscow Region, Russia, September, 2011.

CONCLUSIONS

- The robust procedures for the synthesis of nanogels were developed.
- Key structural parameters of block copolymers governing the physicochemical properties of the nanogels were identified.
- The nanogels loaded with combination of anticancer therapeutics were developed.
- The methods for the preparation of ErbB2-targeted nanogels were developed.
- Mannose functionalized BICs provide a safe and stable platform for gene delivery to macrophages.
- We demonstrated that doxorubicin-nanogels showed an efficient systemic delivery of the drug to human tumor xenografts.

REFERENCES

1. S. Bontha, A.V. Kabanov, T.K. Bronich, Polymer micelles with cross-linked ionic cores for delivery of anticancer drugs, *J. Control. Release* 2006, 114, 163–174
2. T.K. Bronich, P.A. Keifer, L.S. Shlyakhtenko, A.V. Kabanov, Polymer micelle with cross-linked ionic core, *J. Am. Chem. Soc.* 2005, 127, 8236–8237

3. J.O. Kim, N.V. Nukolova, H.S. Oberoi, A.V. Kabanov, T.K. Bronich, Block ionomer complex micelles with cross-linked cores for drug delivery, *Polymer Science Series A* 2009, 51, 708-718.
4. Waterhouse, D.N., Tardi, P. G., Mayer, L. D., Bally, M. B., A comparison of liposomal formulations of doxorubicin with drug administered in free form: changing toxicity profiles. *Drug Saf*, 2001. 24, 903-20.
5. Patil, R.R., Guhagarkar, S.A., Devarajan, P.V., Engineered Nanocarriers of Doxorubicin: A Current Update. *Crit Rev Ther Drug Carrier Syst*, 2008, 25, 1-61.
6. Lu, W.-L., Qi, X-R., Zhang, Q., Li, R-Y., Wang, G-L., Zhang, R-J., A Pegylated Liposomal Platform: Pharmacokinetics, Pharmacodynamics, and Toxicity in Mice Using Doxorubicin as a Model Drug. *J Pharmacol Sci*, 2004, 95, 381-389.
7. Allen, T.M., Hansen, C.B., de Menezes, D.L, Pharmacokinetics of long-circulating liposomes *Adv Drug Delivery Rev*, 1995, 16, 267-284.